LEAST SQUARES IMAGE MATCHING: A COMPARISON OF THE PERFORMANCE OF ROBUST ESTIMATORS

Commission VI, WG VI/4

KEY WORDS: Least Squares Image Matching, Robust Estimators, Accuracy, Comparison, Systematic Errors, Outliers

ABSTRACT:

Least squares image matching (LSM) has been extensively applied and researched for high matching accuracy. However, it still suffers from some problems. Firstly, it needs the appropriate estimate of the initial value. However, in practical applications, initial values may contain some biases from the inaccurate positions of keypoints. Such biases, if high enough, may lead to the solution divergence. If all the tentative matching biases have exactly the same magnitude and direction, then they can be regarded as systematic errors. Secondly, malfunction of an imaging sensor may happen, which generates dead or stuck pixels on the image. This can be referred as outliers. Because least squares estimation is well known for its inability to resist outliers. All these mentioned deviations from the model determined by LSM cause a matching failure. To solve these problems, a variety of robust estimation methods including RANSAC-based method, M estimator, S estimator and Modified M (MM) estimator is applied and compared in the simulation experiments where two scenarios involved with systematic errors and outliers are considered. In addition, an evaluation criterion directly connected with the matching result is proposed to compare these robust estimators. It is found that robust estimators show the robustness for these deviations compared with the commonly LSM. Among these the robust estimators, M and MM estimator have the best performances.

1. INTRODUCTION

Image matching is an active research field in digital photogrammetry and computer vision. The main task in image matching is to find the corresponding pixel on two images of the same physical region. Usually the two images are referred as the reference image and the querying image respectively. In general, this is one fundamental step of various vision-based applications such as camera calibration, panorama generation, object recognition, structure from motion (SFM), 3D map generation and vision-based navigation.

Different matching methods such as keypoint matching and area-based matching are proposed by many researchers. Among them, least squares image matching (LSM) is still attractive for its definite mathematical description of the two patches and high accuracy. Its creation can be traced back to the 1980s when Förstner (1982) firstly put forward the basic idea for LSM. Now the most widely used LSM utilises the intensity as the observation, and combines affine transformation model and linear radiometric model. Since it is a nonlinear model, Taylor expansion transfers the nonlinear model into the linear one to find the solution through iterations. At the same time, because the number of observations exceeds that of unknown parameters, the solution can be obtained in a least squares sense. Finally, an accurate matching is acquired by the solution. Thus, LSM in essence is one process of nonlinear regression.

For its high matching accuracy and good quality monitoring, it has been widely researched and explored to enhance its adaptability and performance. For example, Bethmann and Luhmann (2011) employed the new projective transformation model in the functional model to improve the adaptability. In terms of the stochastic model, most researchers assumed that the measurements involved had equal precision and statistically independent, thus the weight matrix was a diagonal matrix. However, Wu et al. (2007) adapted the stochastic model by Blue estimator and the result showed that the new stochastic model improved matching accuracy by 0.2-0.4 pixel.

Acting as a matching refinement method, LSM has been widely applied in different photogrammetric software. For example, Zhang et al. (2011) performed the pyramid-based LSM to improve the accuracy on low-attitude images acquired by remotely piloted aerial vehicles. Ultimately a 3D city model was generated. Debella-Gilo and Kääb (2012) applied LSM in the surface displacement and deformation of mass movement and showed that LSM matches the images and computes longitudinal strain rates, transverse strain rates and shear strain rates reliably with mean absolute deviations in the order of 10^{-4} as evaluated on stable grounds.

However, LSM still suffers from the divergence problem, which means that the solution from LSM will not promise an accurate result in the end. According to Bethmann and Luhmann (2011), the five aspects will affect the solution of LSM, which are the texture, the reference windows, geometric distortions the quality of initial values, and the functional model.

This paper focuses the research on robust estimation to eliminate the influence of derivations from the LSM model. Two sources are presented. Firstly, the initial values of the unknown parameters are important since the linearization of LSM is based on Taylor expansion. If the initial values of the unknown parameters are not close enough to the correct solution, the error caused by linearization will be large, resulting in a matching failure in the end. However, according to Baine and Rattan (2012), compared with their corresponding points in the reference image, if all the corresponding points in the querying image have a constant bias with the same magnitude and direction, the biases can be classified as systematic errors. Thus, this paper simulates this special case for LSM applications.

Secondly, another type of deviation—Salt & Pepper noise—is considered in this paper. It models the malfunction of the imaging sensor, and simulates other common conditions such as poor illumination, signal transmission and high temperature.

Since LSM already defines the model for the data, which means that the "normal" data pattern has been determined. If one set of data is "faraway" from the main part of the data, it can be identified as deviations. Generally, if the deviation is not large enough, there will be a tiny influence on the final result. However, if it is sizable, it can be identified as an outlier, causing masking and swamping effect, thus it will affect the final solution for linear or nonlinear estimations.

It is well known that the estimation in LSM is least squares estimation, which does not have the resistance to even one outlier. Additionally, multiple outliers rather than one outlier are in existence with a higher possibility. To deal with this problem, one method is to detect and exclude the outliers based on some criterions such as Hadi potential (Hadi, 1992), elliptic norm (Cook and Weisberg, 1982) and Atkinson's distance (Anscombe, 1963). Another method is robust estimation which involves all the observations but reduce the influence of underlying outliers. In this paper, varieties of robust estimators, such as M estimator and S estimator, replace the traditional estimation method (least squares estimation) in LSM, and are compared in terms of the success rate, which is one measurement for all the simulated corresponding points.

There have been extensive studies concerning the comparison on different robust estimators. Knight and Wang (2009) made the comparison of robust estimators on simulated GPS measurements in terms of the ability of outlier exclusion. They demonstrated that no method could correctly exclude all the outliers. For the single outlier, the highest performance is obtained by Modified M estimator (MM) and L_1-norm. Ge et al (2013) made the comparison of 13 commonly used robust estimation methods in the GPS coordinate transformation of the four- and seven-parameter models. With the simulated experiment which controls the different coincident points and the number of gross errors, they showed that L1 and German-McClure method are relatively more efficient.

To the best of our knowledge, the comparison of robust estimator under the situation of systematic errors and outliers for LSM has not been analysed. Therefore, it is the focus of this paper. The rest of this paper is organized as follows. The brief introduction of LSM is presented in Section 2, and the description of outlier sources is proposed in Section 3. Concerning this issue, we introduce robust estimators in Section 4, and then a simulated experiment is conducted in Section 5. Finally, the concluding remarks in Section 6 summarize the outcome of the experiment and describe possible directions of research in LSM in the future.

2. LEAST SQUARES IMAGES MATCHING

Although LSM has been improved in terms of the functional model and the stochastic model for better performance and adaptability, the most common LSM will be briefly introduced in this section as the foundation for further discussions later in this paper.

As an area-based matching method, LSM firstly defines the relationship between two patches with the same size in two images. It takes advantage of the affine transformation model to describe the geometry and the linear model to describe the intensity variation as shown in Equation 1.

$$g_1(x_1, y_1) = h_0 + h_1 g_2(a_0 + a_1 x_1 + a_2 y_1, b_0 + b_1 x_1 + b_2 y_1) \quad (1)$$

where g_1, g_2 = the intensity of the reference image and the querying image respectively. They all depend on the image coordinate x and y
a_i, b_i = the unknown parameters in the affine transformation model
h_0, h_1 = the unknown parameter in the linear model of intensity

However, the solution cannot be acquired directly since it is a nonlinear function, therefore with the help of Taylor expansion it is transformed to a linear one as illustrated in Equation 2.

$$\begin{aligned} & g_1(x_1, y_1) - h_0 - h_1 g_2(x_2, y_2) \\ &= dh_0 + g_2(x_2, y_2)dh_1 + h_1 \frac{\partial g_2}{\partial x_2} da_0 + h_1 x_1 \frac{\partial g_2}{\partial x_2} da_1 \\ &\quad + h_1 y_1 \frac{\partial g_2}{\partial x_2} da_2 + h_1 \frac{\partial g_2}{\partial y_2} db_0 + h_1 x_1 \frac{\partial g_2}{\partial y_2} db_1 \\ &\quad + h_1 y_1 \frac{\partial g_2}{\partial y_2} db_2 \end{aligned} \quad (2)$$

The intensity and coordinates of all corresponding pixels from the two patches are grouped together in the form of Equation 2. Hence a design matrix and its corresponding observations are formed. Generally the number of observations exceeds the undetermined parameters. Thus, traditionally it can be solved by least squares estimation. Finally the iterative process is applied to acquire the final results. However, the iteration needs the terminating criterion, which is usually judged by correlation coefficient between the two patches, or the norm of the corrections is less than a certain small threshold.

3. SOURCES OF DEVIATIONS IN LSM

Under the condition that the two models that describe the geometry and intensity variation respectively of LSM are correct, the inconsistency or deviation with the models will cause unexpected outcomes. Provided that the data set, which includes both the creation of the design matrix and the observation according to the intensity and coordinates in the patch, cannot appropriately fit the model determined by LSM, LSM will not converge to a correct solution, causing mismatches in the end.

To figure out the reason why sometimes LSM cannot work properly, to the best of our knowledge, the two kinds of sources, which are systematic errors and outliers, are presented and analysed.

3.1 Systematic Errors (Initial Bias)

As noted above, LSM is essentially based on Taylor expansion, which needs the appropriate estimation on the initial value of the solution. In other words, these estimations have to be close enough to the solution. Therefore, to obtain the solution in the affine transformation model, the tentative keypoints need to be matched as accurately as possible.

However, for the practical situation such as the commonly used method RANSAC and keypoint matching, when the keypoints are extracted and matched before going through RANSAC with the affine transformation model, they still have re-projection errors which are the basis for setting the threshold of inliers and outliers. Although the error can be controlled with a stricter threshold, it still faces the shortage of available corresponding keypoints in some circumstance. For example, in the following stereo images taken from UAV (Figure 2), SURF (Bay et al., 2006) and BRISK (Leutenegger et al., 2011) points are

extracted and matched, then filtered by RANSAC. If the threshold is set from 1 pixel to 6 pixels, the number of the available keypoints shows a decreasing trend as demonstrated in Figure 3. At the same time, it is an example of the existence of initial biases on image matching.

(a) The image A taken by a UAV

(b) The image B taken by a UAV

Figure 1. The stereo images taken by a UAV

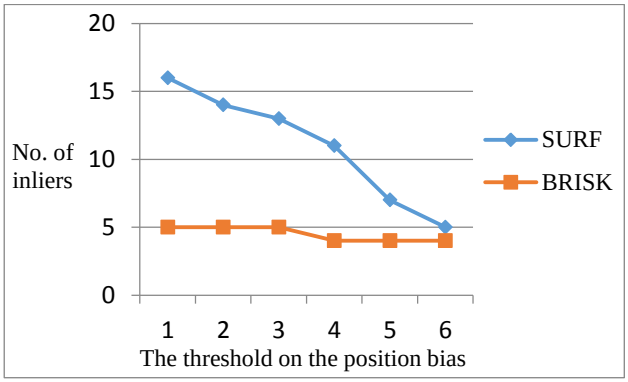

Figure 2. The variation on the number of inliers with different thresholds

If all the biases of the keypoints position have the same magnitude and direction, it denotes the systematic error on matching accuracy, which is considered by the simulation in Section 5.

3.2 Outliers (Imaging Sensor Malfunction)

This relates to the fault in the imaging sensor. A few pixels in the COMS or CCD sensor will not function properly, commonly resulting in dead or stuck pixels on the generated image. However, this rarely happens to the professional photogrammetric cameras since they are strictly tested and excluded by the manufacturer. Nevertheless, in terms of consumer-level cameras, a limited number of pixels (usually 3 at most for the entire pixels in the sensor) are allowed to exist in by the manufacturer considering the cost. Thus, this will also lead to the error on the observation (intensity) in LSM though the chances are very low. These pixels statistically can be identified as outliers.

The imaging sensor malfunction can be modified as Salt & pepper noise, which is illustrated in Equation 3.

$$y(i,j) = \begin{cases} 255 & with\ probability\ of\ p/2 \\ 0 & with\ probability\ of\ p/2 \\ x(i,j) & with\ probability\ of\ 1-p \end{cases} \quad (3)$$

where x = the intensity of the noise-free image
y = the intensity of the image with noises
p = the percentage of affected pixels

Usually the traditional method to deal with this kind of noise is to denoise the contaminated image with various filters such as Mean filter, Gaussian filter and so on (Bovik, 2005). However, in this paper, it is processed from the perspective of data processing and optimal estimation. Salt & Pepper noise acts as the noise model when there are faults in the imaging sensor, thus least squares estimation is heavily affected and cannot be optimal. Thus the application of robust estimation is explored in the next section.

4. ROBUST ESTIMATION

Since LSM possibly involve deviations from various sources as mentioned above, it is highly necessary to get rid of the influence of deviations is. In this section, we will briefly introduce four categories of robust estimation method: RANSAC-based method, M estimator (Reweighting-based method), S estimator and MM estimator.

4.1 Ransac-based Methods

Least median of squares (LMedS) (Rousseeuw, 1984) tries to find the smallest value for the median of squared standardized residuals for the entire data set as shown in Equation 4, while least absolute deviations (LAD) (Powell, 1984), which is also known as $L1$ norm (Equation 5), tries to minimize the sum of absolute standardized residuals. There are a number of methods to find the minimum of the two objective functions. However, RANSAC is simply applied to research the entire data and find out the solution.

$$min(median(r^2)) \quad (4)$$

$$min \sum_{i=1}^{n} |r_i| \quad (5)$$

where r = the standardized residual

An important parameter for RANSAC is the percentage of outliers or the inliers, which define the minimum number of iterations, which is shown in Equation 6. In this paper, the percentage of inliers is assumed to be 0.5. Besides, p and n are set to be 0.95 and 8 respectively.

$$k = \frac{log(1-p)}{log(1-w^n)} \quad (6)$$

where p = the success rate of RANSAC
w = the percentage of inliers
n = the number of observations to acquire the solution

4.2 M Estimator (Reweighting-based Method)

M estimator is another common method for robust estimation. Instead of minimizing $\sum_{i=1}^{n} r_i^2$, these reweighting-based M estimators tries to minimize $\sum_{i=1}^{n} \rho(r_i)$, where $\rho(r_i)$ is less increasing than the square function in least squares estimation, and it is a symmetric, positive-define function with only one unique minimum at zero. However, in practice, we make use of the weighting functions, which is the second derivative of $\rho(r_i)$. The detailed derivation can be found in the book of James (2005). The following equations are the weighting functions for standardized residuals. All r and c in the following equations represent the standardized residuals of the least squares solution and the turning value respectively.

(a) Huber Method (Huber, 1981)

$$w(r) = \begin{cases} 1 & |r| \le c \\ \frac{c}{r} & |r| > c \end{cases} (c = 1.3450) \quad (6)$$

(b) Andrews Method (Andrews, 1974)

$$w(r) = \begin{cases} 1 & |r| = 0 \\ 0 & |r| > c\pi \ (c = 1.3390) \\ c\frac{\sin(r/c)}{r/c} & |r| \le c\pi \end{cases} \quad (7)$$

(c) Welsch Method (Holland and Welsch, 1977)

$$w(r) = \begin{cases} 1 & |r| = 0 \\ 0 & |r| > c\pi \ (c = 1.3390) \\ c\frac{\sin(r/c)}{r/c} & |r| \le c\pi \end{cases} \quad (8)$$

(d) Fair Method (William, 1983)

$$w(r) = \frac{1}{1+\frac{|u|}{c}} (c = 1.3998) \quad (9)$$

(e) Cauchy Method

$$w(r) = \frac{1}{1+(\frac{|u|}{c})^2} (c = 2.3849) \quad (10)$$

4.3 S Estimator

S estimator tries to minimise the dispersion of the residuals, According to Rousseeuw and Leroy (1987), it tries to minimise

$$\frac{1}{n}\sum_{i=1}^{n} \rho(\frac{r_i}{s}) = K \quad (11)$$

where the appropriate weighting function ρ satisfies the following conditions:

(a) ρ is a symmetric and continuously differentiable function, and $\rho(0) = 0$.

(b) ρ is strictly increasing on $[0, a]$ and constant on $[a, \infty)$.

(c) $\frac{K}{\rho(a)} = \frac{1}{2}$

Since S estimator is computationally expensive, S estimator with Fast-S algorithm is applied in this paper. Its detailed process can be found in Salibian-Barrera and Yohai (2006).

4.4 Modified M Estimator

Modified M (MM) (Yohai, 1987) estimator makes use of S estimator to obtain the initial estimate, and the residuals acquired from S estimator can be used to determine the scale factor of M estimator. With the scale factor, an iteratively reweighted least squares procedure like that of M estimator is implemented to acquire the final solution. In this paper, to reduce the computational burden, Fast S (Salibian-Barrera and Yohai, 2006) estimator is applied for the initial estimate.

5. SIMULATION EXPERIMENTS

The convergence of LSM is related to image texture, but it is difficult to control the texture. Therefore this paper presents a set of images for different environments to reduce the bias of the testing data. They are three images taken by a low altitude UAV and one image of Mars surface taken by NASA's Mars Reconnaissance Orbiter (MRO), which are all listed sequentially in Figure 3.

(a) The image 1 taken by a UAV

(b) The image 2 taken by a UAV

(c) The image 3 taken by a UAV

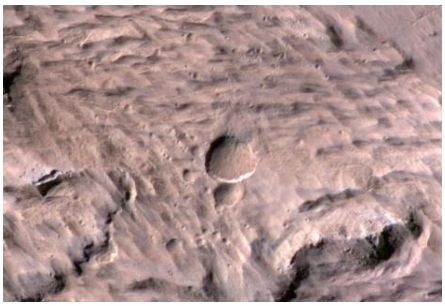

(d) The image 4 taken by Mars Reconnaissance Orbiter

Figure 3. The testing images

Since in the real practice, the exact positions of the corresponding points in the reference image and the querying image are never known, therefore the accuracy has to be evaluated with some indicator such as correlation coefficient based on the intensity of two patches. However, another way to evaluate the accuracy is to simulate corresponding points. Because the exact positions of the corresponding points in the querying image and the reference image as well as their geometry are known, the matching accuracy can be evaluated.

To generate the simulated corresponding point in the reference image, four nets consisting of such points are created with different intervals. The numbers of simulated corresponding points for the four images are different since the images have different width and length except the image 2 and 3. The detailed information about the four images is shown in Table 1.

Images / Trait	UAV1	UAV2	UAV3	Mars
No. of Points	450	609	609	486
Resolution Ratio	4000×3000	4608×3456	4608×3456	1413×951

Table 1. The characteristics of the four images

For the generation of "simulated" points in the querying image, a special affine transformation model is applied, which is

$$\begin{pmatrix} 1 & 0 & 0 \\ 0 & 1 & 20 \\ 0 & 0 & 1 \end{pmatrix} \quad (12)$$

Actually the simulation degenerates to a translation model that avoids scaling and rotational variation. Besides, there are no occlusions in the simulated querying image. It should be noted that this is often the case for the epipolar image, which is commonly used for stereo matching and digital elevation model (DSM) generation. Besides, the epipolar image can be generated from non-epipolar image by image rectification. Therefore it is still reasonable to apply this model.

Finally, four image pairs are produced from the four testing images. For instance, as show in the Figure 4, there is a 20-pixel-wide strip in its simulated image, which means that all the simulated points are translated towards the right direction for 20 pixels.

Figure 4. The image 1 (the reference image) and its simulated image (the querying image)

It should be noted that a terminating criterion is applied in the iteration of LSM in the simulation experiment. That is when the parameters in the affine transformation model lead to the overflow from the boundary. This means that LSM has already failed.

To evaluate the accuracy of the final result from LSM, the final corresponding coordinates of the simulated points are employed from LSM instead of checking correlation coefficient, since a higher correlation coefficient does not necessarily reflect the higher matching accuracy, therefore, according to the affine transformation model in Equation 12, the final accuracy can be calculated by using Equation 13.

$$\sqrt{(x_{Re} - x_{Qu} + 20)^2 + (y_{Re} - y_{Qu})^2} \quad (13)$$

where x and y are the final coordinate of the simulated corresponding points. If the value obtained from Equation 13 is less than 0.001 pixel, it is counted as an accurate matching pair. Besides, we count the number of tentative matching pairs that pass the terminating criterion, if the total number of accurate matching pair, which is the number of matching pair that passed Equation 13 divided by the total number of tentative matching pair, a ratio can be acquired. This means the success rate for LSM. In addition, the size of the template is 17×17 pixels and the maximum number of iterations is 10.

5.1 Test on Systematic Errors

Different levels initial matching biases (from 1 pixel to 3.5 pixels) on the tentative matching pairs are added on the simulated corresponding points. The results from different estimators are shown in Table 2-5.

Bias / Method	0.5 pixel	1 pixel	1.5 pixels	2 pixels	2.5 pixels	3 pixels
OLS	99.56%	**100.00%**	99.11%	85.11%	84.00%	70.89%
LMedS	98.89%	95.33%	85.11%	57.56%	50.00%	0.00%
LAD	93.33%	88.89%	83.78%	53.78%	44.89%	25.33%
Huber	**100.00%**	**100.00%**	**99.78%**	89.56%	88.44%	77.56%
Andrews	**100.00%**	**100.00%**	**99.78%**	**89.78%**	88.89%	79.56%

Welsh	**100.00%**	**100.00%**	**99.78%**	89.56%	**90.22%**	**80.22%**
Fair	**100.00%**	**100.00%**	**99.78%**	89.33%	88.22%	76.89%
Cathay	**100.00%**	**100.00%**	**99.78%**	89.56%	89.11%	78.00%
FastS	99.56%	99.56%	99.11%	88.89%	84.67%	69.33%
MM	**100.00%**	**100.00%**	**99.78%**	**89.78%**	89.33%	79.56%

Table 2. The success rate for the image pair 1 with systematic error

Bias / Method	0.5 pixel	1 pixel	1.5 pixels	2 pixels	2.5 pixels	3 pixels
OLS	**100.00%**	**100.00%**	99.51%	68.31%	59.28%	38.59%
LMedS	97.87%	90.64%	75.86%	33.83%	21.51%	6.4%
LAD	93.92%	89.33%	75.04%	37.77%	22.66%	6.08%
Huber	**100.00%**	**100.00%**	99.67%	73.40%	66.01%	44.99%
Andrews	**100.00%**	**100.00%**	**99.84%**	73.40%	66.50%	45.48%
Welsh	**100.00%**	**100.00%**	99.67%	**74.88%**	66.01%	46.31%
Fair	**100.00%**	**100.00%**	99.67%	73.23%	65.52%	45.65%
Cauthy	**100.00%**	**100.00%**	**99.84%**	73.89%	66.17%	**47.45%**
FastS	99.84%	99.84	99.01%	73.23%	61.08%	34.32%
MM	99.84%	**100.00%**	99.67%	73.56%	**66.67%**	45.16%

Table 3. The success rate for the image pair 2 with systematic error

Bias / Method	0.5 pixel	1 pixel	1.5 pixels	2 pixels	2.5 pixels	3 pixels
OLS	99.67%	99.51%	97.04%	69.79%	56.81%	36.62%
LMedS	97.21%	93.27%	77.34%	38.26%	23.15%	11.00%
LAD	82.27%	69.62%	49.10%	20.36%	9.85%	3.28%
Huber	**99.84%**	**99.67%**	97.37%	72.58%	61.41%	41.22%
Andrews	**99.84%**	99.34%	97.04%	**73.07%**	59.77%	40.39%
Welsh	99.67%	99.51%	97.21%	72.91%	61.41%	41.38%
Fair	99.67%	**99.67%**	97.37%	72.91%	**62.07%**	41.38%
Cauthy	99.67%	99.51%	**97.54%**	72.91%	**62.07%**	41.38%
FastS	97.54%	97.70%	94.58%	71.10%	55.99%	32.02%
MM	98.69%	98.85%	96.55%	72.58%	60.43%	**42.04%**

Table 3. The success rate for the image pair 3 with systematic error

Bias / Method	0.5 pixel	1 pixel	1.5 pixels	2 pixels	2.5 pixels	3 pixels
OLS	96.71%	98.15%	95.47%	89.09%	84.16%	61.73%
LMedS	28.19%	16.46%	16.05%	5.56%	4.53%	1.85%
LAD	7.61%	4.53%	2.88%	1.44%	0.41%	0.21%
Huber	**97.74%**	**99.59%**	96.09%	90.53%	**86.42%**	64.61%
Andrews	96.50%	98.15%	95.27%	88.68%	83.74%	62.35%
Welsh	97.53%	99.18%	95.88%	89.92%	85.60%	64.20%
Fair	**97.74%**	**99.59%**	**96.71%**	**91.56%**	**86.42%**	**65.84%**
Cauthy	97.12%	**99.59%**	96.30%	90.53%	86.21%	**65.84%**
FastS	83.33%	83.33%	75.51%	62.55%	54.12%	38.48%
MM	96.71%	97.74%	94.03%	88.48%	83.74%	62.76%

Table 5. The success rate for the image pair 4 with systematic error

The results from the test of the four images show that, with the increase of systematic errors, generally the success rates of all the estimation methods have decreasing trends, excepts that the success rate slightly increases when the systematic error changes from 0.5 pixel to 1 pixel. When the systematic error is around 1 pixel, ordinary least squares (OLS) can maintain the success rate at nearly 100%. Nevertheless, when the systematic error increases to 3 pixels, OLS can hardly keep up the success rate as it is heavily influenced by the deviation from the model of LSM. However, at the same time, other robust estimators show the robustness in dealing with the systematic error compared with OLS.

The resistance to the systematic error is achieved by these robust estimators as it can be observed from the highest success rate labelled in Table 2-5. Firstly, the performances of RANSAC-based methods are not stable. For the image 1, 2 and 3, they have a comparative performance with other estimators. However, they have a much lower success rate in the image 4. One possible reason lies in the texture of image 4, which leads to different design matrixes and observations.

The result from Fast S estimator is not stable. For the first three images, it keeps the similar performance with OLS. But sometimes its success rates are still lower than OLS especially when the systematic error is 3 pixels. One possible reason is that it wrongly eliminates the influence of some good observations fitting the model.

M estimator and MM estimator have stable and best performances for all the images compared with other estimators. As they can be observed from the labelled value in Table 2-5, when the systematic error is small, they obtain almost all the highest success rate. Likewise, when the systematic error is larger, they still maintain satisfactory performances. Especially when the pixel error is 3 pixels, M estimator including Cauthy, Welsh and Fair as well as MM estimators have the best performance.

5.2 Test on Systematic Errors and Outliers

Systematic errors were set from 0.5 pixel to 1.5 pixels since the focus is the robustness to outliers under normal conditions. Outliers were introduced in this test, and the noise level on each image, which is the percentage of malfunctioning pixels in the imaging sensor, was set at 0.1%, 0.5% and 1% respectively. More extreme conditions with a higher noise level were not tested in this section since they rarely happen in the actual application. Besides, all the simulated corresponding points from the four images were added together as a whole to evaluate the overall performance of various robust estimators under different noise levels.

Bias / Methods	0.5 pixel	1 pixel	1.5 pixels
OLS	76.97%	76.46%	74.88%
LMedS	81.57%	75.49%	65.69%
LAD	76.66%	70.01%	60.82%
Huber	99.35%	98.05%	97.08%
Andrews	99.12%	99.30%	97.96%
Welsh	**99.44%**	99.30%	98.10%
Fair	98.38%	95.87%	94.94%
Cauthy	99.30%	**99.49%**	**98.38%**
FastS	95.68%	95.13%	92.53%
MM	98.93%	99.12%	97.63%

Table 6.The success rate with noise level 0.1%

Bias / Methods	0.5 pixel	1 pixel	1.5 pixels
OLS	27.21%	25.63%	24.98%
LMedS	81.34%	75.30%	66.16%
LAD	75.12%	67.73%	56.04%
Huber	94.66%	86.54%	86.77%
Andrews	97.96%	96.84%	95.73%
Welsh	98.42%	96.05%	95.64%
Fair	89.60%	77.76%	77.16%
Cauthy	97.31%	94.29%	92.99%
FastS	95.17%	95.59%	92.71%
MM	**98.93%**	**99.03%**	**97.45%**

Table 7.The success rate with noise level 0.5%

Bias / Methods	0.5 pixel	1 pixel	1.5 pixels
OLS	7.61%	6.69%	6.31%
LMedS	81.38%	74.56%	63.51%
LAD	67.87%	57.29%	46.33%
Huber	81.57%	66.48%	67.04%
Andrews	94.71%	89.00%	89.83%
Welsh	89.14%	80.55%	80.22%
Fair	72.10%	56.04%	56.17%
Cauthy	89.88%	81.75%	81.34%
FastS	95.68%	94.71%	93.18%
MM	**98.75%**	**98.38%**	**96.84%**

Table 8. The success rate with noise level 1%

As it can be observed from Table 6-8, when the noise level is 0.1%, the success rates of OLS drop dramatically. And the declining trend continues with the increase of the noise level. When it reaches to 1%, the success rates of OLS are around 7%, which means that OLS cannot work properly in this scenario.

The other robust estimators show good performances compared with OLS. When the noise level is 0.1%, the two RANSAC-based methods—LMed and LAD—almost have equal performance with OLS. Nonetheless, the increase of the noise level, they begin to show the robustness. Yet they still have the lower performances compared with other robust estimators such as M and MM estimator.

Fast S estimator generally has comparative performance with other estimators as they can maintain the success rate above 90%.

From the labelled success rate in Table 6-8, M and MM estimators obtain the best performance, and success rates remain at above 95%.

6. CONCLUDING REMARKS

Four categories of robust estimation method including RANSAC-based method, M estimator, S estimator and MM estimator are applied and compared as the estimation methods LSM. Therefore some concluding remarks can be made. Firstly, it is found that the initial bias on LSM should be controlled within 1.5 pixels to maintain the high performance. Secondly M and MM estimators have higher abilities to eliminate the influence of deviations than other methods, thus when both the initial bias and image quality are unknown, the two robust estimators provide comparative and safe alternatives of OLS.

To linearize a nonlinear function for parameter estimation, the convergence also has the relationship with the function itself. Similarly, the model determined by LSM is a function about the intensity that depends on the image coordinate and y, and other related coefficients, which directly comes from the texture of the image. Therefore the convergence of LSM is linked with the texture. However, if the nonlinearity of the model in LSM does not allow the linearization, LSM will not converge to a correct solution. But how nonlinearity is linked with the image texture remains a problem that needs to be further explored.

ACKNOWLEDGEMENTS

The first author is sponsored by China Scholarship Council (CSC) for his PhD studies at UNSW Australia. Sincerely thanks go to Dr. Yincai Zhou and Dichen Liu for providing the UAV images, as well as Joossens K for providing the related Matlab function.

REFERENCES

Andrews, D. F., 1974. A robust method for multiple linear regression. *Technometrics*, 16(4), pp. 523-531.

Anscombe, F. J., Tukey, J. W., 1963. The examination and analysis of residuals. *Technometrics*, 5(2), pp. 141-160.

Baine, N. A., Rattan, K. S., 2012. Algorithm for the detection and isolation of systemic measurement errors in vision based/aided navigation systems. In: *2012 IEEE/ION Position, Location and Navigation Symposium*, Myrtle Beach, SC, USA, pp. 366-370.

Bay, H., Tuytelaars, T., Van Gool, L., 2006. Surf: Speeded up robust features. In: *2006 European Conference on Computer Vision*, pp. 404-417.

Bethmann, F., Luhmann, T., 2011. Least-squares matching with advanced geometric transformation models. *Photogrammetrie-Fernerkundung-Geoinformation*, 2011(2), pp. 57-69.

Bovik, A. C., 2005. *Handbook of Image and Video Processing*. Elsevier Academic Press.

Cook, R. D., & Weisberg, S. 1982. *Residuals and Influence in Regression*. CHAPMAN and HALL.

Debella-Gilo, M.; Kääb, A., 2012. Measurement of surface displacement and deformation of mass movements using least squares matching of repeat high resolution satellite and aerial images. *Remote Sensing*, 4(1), pp. 43-67.

Förstner, W., 1982. On the geometric precision of digital correlation. *International Archives of Photogrammetry and Remote Sensing*, 24(3), pp. 176-189.

Ge, Y., Yuan, Y., Jia, N., 2013. More efficient methods among commonly used robust estimation methods for GPS coordinate transformation. *Survey Review*, 45(330), pp. 229-234.

Hadi, A. S., 1992. A new measure of overall potential influence in linear regression. *Computational Statistics & Data Analysis*, 14(1), pp. 1-27.

Holland, P. W., Welsch R. E., 1977. Robust regression using iteratively reweighted least-squares. *Communications in Statistics: Theory and Methods*, pp. 813–827.

Huber, P. J., 1981. *Robust Statistics*. John Wiley, New York.

Knight, N. L., Wang, J., 2009. A comparison of outlier detection procedures and robust estimation methods in GPS positioning. *Journal of Navigation*, 62(04), pp. 699-709.

Leutenegger, S., Chli, M., Siegwart, R. Y., 2011. BRISK: Binary robust invariant scalable keypoints. In: *2011 IEEE International Conference on Computer Vision*, pp. 2548-2555.

Powell, J. L., 1984. Least absolute deviations estimation for the censored regression model. *Journal of Econometrics*, 25(3), pp. 303-325.

Rousseeuw, P. J., 1984. Least median of squares regression. *Journal of the American Statistical Association*, 79(388), pp. 871-880.

Rousseeuw, P. J., Leroy, A. M., 1987. *Robust Regression and Outlier Detection*. Wiley, Hoboken.

Salibian-Barrera, M., Yohai, V. J., 2006. A fast algorithm for S-regression estimates. *Journal of Computational and Graphical Statistics*, 15(2).

William, J. J. R., 1983. *Introduction to Robust and Quasi-Robust Statistical Methods*. Springer, Berlin.

Wu, J., Zhang, Q., Wang, J., 2007. Least squares image matching and precision improvement. *Journal of Photogrammetry and Remote Sensing*, 12(3), pp. 217-224.

Yohai, V. J., 1987. High breakdown point and high efficiency robust estimates for regression. *The Annals of Statistics*, 15, pp. 642–656.

Zhang, Y., Xiong, J., Hao, L., 2011. Photogrammetric processing of low altitude images acquired by unpiloted aerial vehicles. *The Photogrammetric Record*, 26(134), pp. 190-211.